



Permafrost carbon emissions in a changing Arctic

Kimberley R. Miner¹✉, Merritt R. Turetsky², Edward Malina¹, Annett Bartsch^{3,4}, Johanna Tamminen⁵, A. David McGuire⁶, Andreas Fix⁷, Colm Sweeney⁸, Clayton D. Elder¹ and Charles E. Miller¹

Abstract | Arctic permafrost stores nearly 1,700 billion metric tons of frozen and thawing carbon. Anthropogenic warming threatens to release an unknown quantity of this carbon to the atmosphere, influencing the climate in processes collectively known as the permafrost carbon feedback. In this Review, we discuss advances in tracking permafrost carbon dynamics, including mechanisms of abrupt thaw, instrumental observations of carbon release and model predictions of the permafrost carbon feedback. Abrupt thaw and thermokarst could emit a substantial amount of carbon to the atmosphere rapidly (days to years), mobilizing the deep legacy carbon sequestered in Yedoma. Carbon dioxide emissions are proportionally larger than other greenhouse gas emissions in the Arctic, but expansion of anoxic conditions within thawed permafrost and soils stands to increase the proportion of future methane emissions. Increasingly frequent wildfires in the Arctic will also lead to a notable but unpredictable carbon flux. More detailed monitoring through in situ, airborne and satellite observations will provide a deeper understanding of the Arctic's future role as a carbon source or sink, and the subsequent impact on the Earth system.

¹Jet Propulsion Laboratory, California Institute of Technology, Pasadena, CA, USA.

²INSTAAR, Department of Ecology and Evolutionary Biology, University of Colorado Boulder, Boulder, CO, USA.

³b.geos, Korneuburg, Austria.

⁴Austrian Polar Research Institute, Vienna, Austria.

⁵Finnish Meteorological Institute, Helsinki, Finland.

⁶Institute of Arctic Biology, University of Alaska Fairbanks, Fairbanks, AK, USA.

⁷Deutsches Zentrum für Luft- und Raumfahrt (DLR), Institut für Physik der Atmosphäre, Oberpfaffenhofen, Germany.

⁸NOAA Global Monitoring Laboratory, Boulder, CO, USA.

✉e-mail: Kimberley.N.Miner@jpl.nasa.gov

<https://doi.org/10.1038/s43017-021-00230-3>

Permafrost underlies ~25% of the Northern Hemisphere land surface and stores an estimated ~1,700 Pg (1,700 Gt) of carbon in frozen ground, the active layer and talik^{1,2}. Rapid anthropogenic warming and resultant thaw threaten to mobilize permafrost carbon stores^{3,4}, potentially increasing atmospheric concentrations of carbon dioxide (CO₂) and methane (CH₄), and converting the Arctic from a carbon sink to a carbon source. This process, and its potential impact on future warming, is known as the permafrost carbon feedback (PCF) to climate^{5,6}. Despite its importance to climate predictions^{1,7}, the PCF remains highly uncertain, and accurate projections of the locations, magnitudes and speeds of permafrost carbon release are lacking. Furthermore, permafrost dynamics are often not included in Earth system models (ESMs).

Since 2015, sediment cores⁸, surface temperature readings⁹ and other proxies^{10,11} have contributed to global permafrost characterization. Upscaling of research and airborne missions have identified the importance of shoulder and cold season emissions, especially in terms of CH₄ (REFS^{12–14}). Most PCF modeling activities have focused on gradual permafrost thaw via active layer thickening. This type of permafrost thaw occurs progressively, with thaw depths increasing a few centimetres per decade^{3,15}, and impacts microbial

activities and rhizosphere priming^{16,17}. However, it is becoming increasingly clear that abrupt thaw processes, such as thermokarst and thermoerosion, could expose many metres of permafrost carbon to mobilization on the timescale of days to a few years^{3,18–20}.

Abrupt thaw can be triggered by climate warming or landscape disturbances, including wildfires or hydrological regime changes^{3,21–23}. In turn, abrupt thaw causes thermal, hydrological and vegetation changes that amplify warming and thaw^{24–27}. As a result, spatial disaggregation expands and landscape morphology changes, mobilizing carbon^{28–30}. The three-dimensional, fine-scale nature of thaw and resulting feedbacks make abrupt carbon release difficult to model or forecast²⁵. Adding to these challenges, unknowns around the future Arctic climate wetting, drying and thaw patterns limit the accuracy of PCF forecasts.

In this Review, we outline progress in understanding permafrost change and the PCF, including dynamics contributing to abrupt thaw in the Arctic system. Permafrost distribution and carbon stocks under anthropogenic warming are reviewed, followed by a discussion of carbon emissions across scales and sources. Finally, research priorities to enable accurate PCF forecasts across the permafrost-affected regions of the high northern latitudes are described.

Key points

- Tundra fire and abrupt thaw events are increasingly driving the release of permafrost carbon into the atmosphere.
- Observational tools improve carbon flux estimates across scales, but scaling remains a major challenge.
- Satellite systems scheduled to come online by 2025 will provide high-frequency data and enable better monitoring of permafrost carbon emissions.
- Earth system models must include permafrost dynamics to enable accurate permafrost carbon feedback projections.

Active layer

In permafrost environments, the top layer of substrate that often freezes in winter and thaws in the spring and summer (less than 50 cm thick in the tundra and up to 3 m in boreal regions).

Talik

A layer of soil that is unfrozen year-round within the permafrost. Often found below lakes, wetlands or rivers.

Permafrost carbon feedback

(PCF). The accelerated release of carbon into the atmosphere from the thawing of the permafrost.

Abrupt thaw

Rapid permafrost thaw that occurs on timescales of a few days to a few years.

Thermokarst

An erosional landscape process of abrupt thaw, resulting in permafrost structural collapse.

Yedoma

Carbon-rich (at least 210 PgC globally), Pleistocene-era permafrost containing up to 90% ice.

RCP4.5

The median Representative Concentration Pathway (RCP) used by the Intergovernmental Panel on Climate Change (IPCC) for climate modelling on the IPCC Fifth Assessment Report in 2014.

RCP8.5

The highest carbon emission scenario Representative Concentration Pathway (RCP) used by the Intergovernmental Panel on Climate Change (IPCC) for climate modelling on the IPCC Fifth Assessment Report in 2014.

Permafrost carbon dynamics

In the past decade, an increased interest in permafrost degradation and the impacts of anthropogenic climate change have facilitated a better understanding of permafrost carbon dynamics. These advances are now highlighted.

Permafrost distribution and carbon stocks. Permafrost currently covers ~30 million km² of the planet⁹. An estimated 13–18 million km² of permafrost is in the Arctic³¹, 1.06 million km² is on the Tibetan Plateau³² and 16–21 million km² is submerged in the subsea³³ (FIG. 1a). However, the underlying depth, structure and status of permafrost remain challenging to quantify³⁴. Cataloguing Pleistocene-aged Yedoma permafrost is particularly difficult, due to its general depth (below >3 m) and thickness (often covering >40 m), with current estimates of its areal extent at ~1 million km² (REF.³⁵). Regardless, understanding its distribution is critical to predicting the future PCF^{35–38}. Yedoma contains up to 90% ice per volume^{3,39} and more carbon than any other permafrost strata per square metre (2–4 wt%; totalling at least 210 PgC globally)^{40,41}. Abrupt degradation disproportionately affects these carbon-rich and ice-rich areas, with thermokarst, hollows and hummocks currently covering ~20% (3.6 million km²) of the Arctic^{1,25}.

In addition to Yedoma carbon stocks, the top 3 m of permafrost soils in the northern circumpolar region cumulatively store an estimated 1,000 PgC (range: –170, +186)⁴². Diverse Arctic vegetation, soils and microorganisms introduce regional variability in both legacy and contemporary carbon stocks across landscapes⁴³, so carbon stocks vary substantially within even small areas. From the local to the landscape scale, soil carbon density estimates vary substantially (17–73%), mirroring the underlying substrate structure⁴⁴.

Warming events in the Arctic have increased in frequency in the past few years^{45,46}, and regional temperature anomalies of up to +40 °C during the deep cold season overlay some of the largest areas of carbon-rich permafrost (>100 kg m^{–2})⁴⁷. Measurements from the Global Terrestrial Network for Permafrost suggest that, between 2007 and 2016, continuous permafrost in the top 3 m throughout the Arctic warmed 0.39 ± 0.15 °C on average⁴⁸ (FIG. 1b), raising concerns about the rapid rate of thaw and potential old carbon release^{5,49–55}. Where peatlands and permafrost overlap, deeply buried carbon within is increasingly at risk from warming, and a substantial loss of Yedoma could potentially result in a 50% increase in the PCF by 2100 (REFS^{35,40,55}). Additionally, while peatlands currently function as a carbon sink,

continued warming could thaw an estimated 0.8 to 1.9 million km² of permafrost peatlands, increasing permafrost carbon release by up to 50%⁵⁶.

Incorporating contemporary warming, model simulations predict a total loss of near-surface permafrost (0–3 m) ranging from 0.2 to 58.8 × 10³ km² per year⁷. This estimate reflects a loss of 3–5 million km² permafrost in the RCP4.5 scenario and 6–16 million km² for RCP8.5 by 2100 (REF.⁵⁷). Subsequently, vulnerable permafrost in the top 3 m is expected to discharge 0.62 PgCO₂ per year (624 million tons) by 2100 through gradual thaw alone^{3,58}.

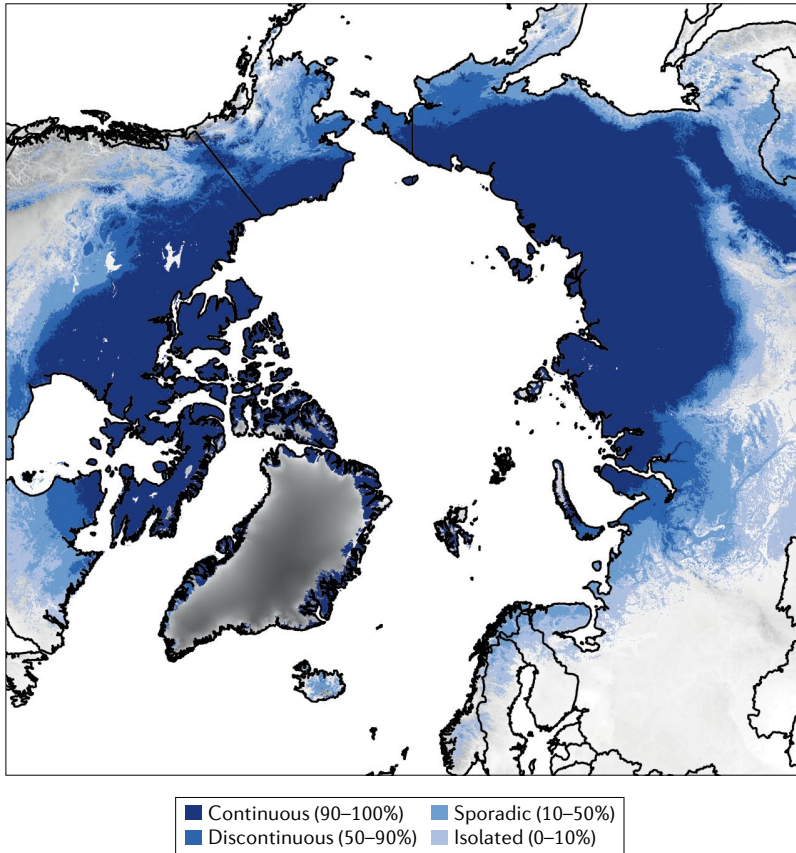
Thermokarst expansion. Increasingly frequent abrupt permafrost thaw events are expected with climate change^{3,55} (FIG. 2). Thermokarst slumps — erosional features associated with abrupt thaw — increased 60-fold between 1984 and 2015 (REFS^{1,59}). While the magnitude of forecasted emissions varies, in situ calculations highlighted the rapid loss of carbon after thermokarst and high CH₄:CO₂ ratios^{16,60}.

Thermokarst thaw lakes⁶¹ now cover 1.095 million km², representing an estimated release of 14–18 TgC per year⁶². Additionally, talik expansion below thermokarst lakes might have already released ~2.5 Pg of legacy (Pleistocene-age) Yedoma carbon, providing a direct route between deep carbon and the atmosphere^{4,35,37}. As permafrost ice structures degrade, meltwater seeks the lowest local elevation, creating spatially disparate frozen and thawed areas at greater risk of thaw^{29,63–65}. Permafrost impacted by abrupt degradation can lose ground ice within 1–3 weeks after snowmelt, maintaining higher temperatures than the surrounding area and thawing rapidly in the spring⁶⁶. Meltwater from abrupt degradation also acts as an efficient lateral transport mechanism, quickly mobilizing carbon.

Landscape hotspots exhibiting abrupt thaw are expected to double to 1.6 million km² by 2100 under RCP8.5, corresponding to emissions of 613–802 TgCO₂e per year, by 2100 (REF.³). These estimates for abrupt thaw expansion would impact only ~1% of the total projected permafrost area, but emissions from this area could grow to 80 ± 19 PgC by 2300 — nearly half of the output expected from gradual thaw³. The potential for abrupt thaw to rapidly release a disproportionate fraction of permafrost carbon is a growing concern¹³.

Owing to the diversity of processes driving it, there is ongoing uncertainty in forecasting abrupt thaw, making it increasingly important to resolve the mechanisms that result in permafrost carbon emissions. The impacts of abrupt thaw are not incorporated into a majority of current PCF models, and, therefore, into few ESMs, substantially increasing uncertainty in estimates of future carbon flux. For example, the high fluxes of contemporary carbon (1950 to present) in Siberian rivers mask the signal of Holocene and Pleistocene carbon released in abrupt thaw⁴¹. Systematic radiocarbon (¹⁴C) measurements of dissolved carbon in Arctic river networks (by the Arctic Great Rivers Observatory, for example) could be used to trace mobilization of carbon from Holocene, Pleistocene and older deposits. Such measurements could provide early warning of abrupt or subsurface permafrost thaw over vast areas. Classifying the lability of deep permafrost

a Permafrost extent



b Temperature change

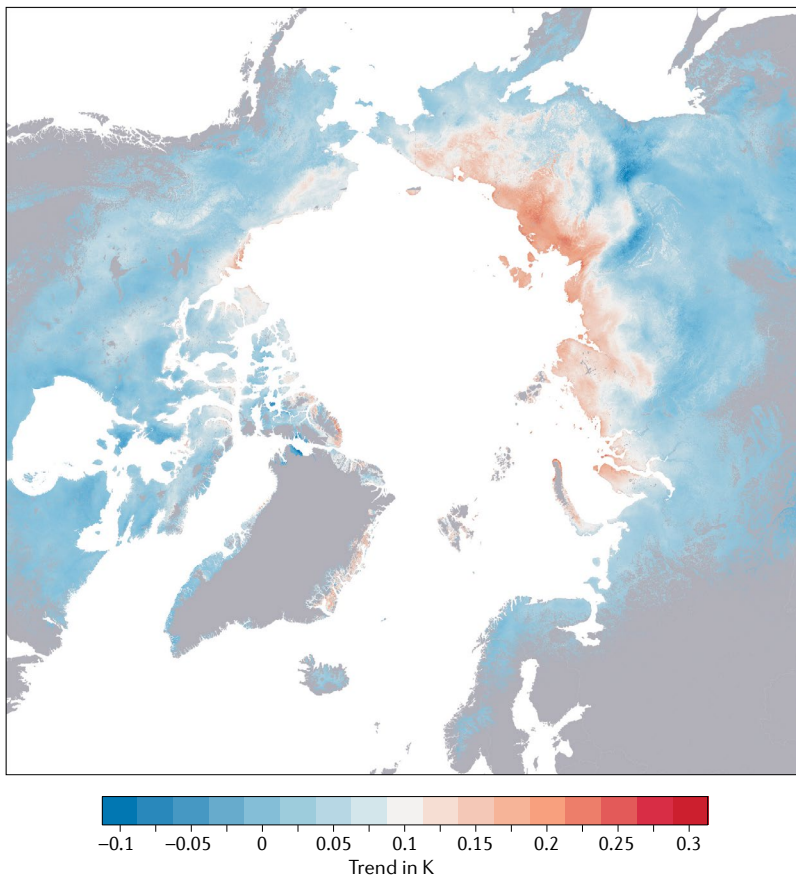


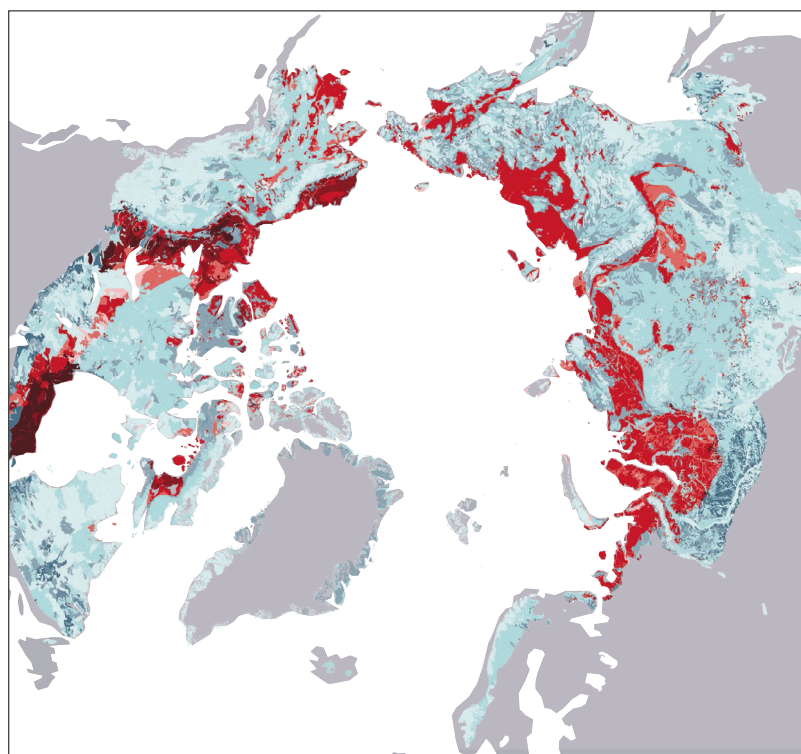
Fig. 1 | Permafrost location and temperature in the Arctic. **a** | Location of permafrost in the Arctic, delineated into continuous, discontinuous, sporadic and isolated¹¹. **b** | Subsurface temperature change at 2 m depth between 1997 and 2018 based on satellite data and thermal modelling¹⁹³. Warming is greatest near the poles, where permafrost ice content is highest and most vulnerable to thaw. Panel **a** adapted from REF.¹⁹⁴, Springer Nature Limited.

carbon and ground ice density is also critical to accurately forecasting the PCF under abrupt thaw^{67–69}.

Microbially mediated emissions. Arctic greenhouse gas emissions are currently dominated by microbially mediated CO₂ release^{70–72}, although thermokarst development could increasingly provide a pathway for greater CH₄ release^{27,73} (FIG. 3). Most current CO₂ and CH₄ fluxes are from carbon sequestered within the last 1,000 years⁷³. While the average Arctic CH₄:CO₂ ratio is 0.2, the current ratio of CH₄:CO₂ emitted from Yedoma thermokarst lakes in Alaska and Siberia is 0.3, with mean annual CH₄ output (129.6 ± 8.6 gCm⁻² per year) lower than mean CO₂ (449.0 gCm⁻² per year)⁵⁵. The ratio from non-Yedoma thermokarst lakes is similar (0.25 CH₄:CO₂), indicating that CO₂ dominates carbon emissions in a variety of Arctic land cover types⁵⁵. However, observed emissions with Pleistocene-aged ¹⁴C could continue to grow as Yedoma thaws. Further estimates suggest that Yedoma could lose an additional 354 ± 196 gCO₂ kgC⁻¹ (C and Ce from oxic and anoxic soils) by 2100 (REF.⁶⁹).

Although anoxic environments typically emit 3.4 times less total carbon than oxic environments, and CO₂ emissions continue to dominate, enhanced CH₄ emissions have ~35 times more warming potential than CO₂ on a 100-year timescale. Therefore, an increase of CH₄ production will have marked impact on the PCF^{74,75}. CH₄ is produced by methanogenic microorganisms in anoxic subsurface environments. Most of the CH₄ is metabolized by methanotrophs, and even a few centimetres of oxic environmental buffering can facilitate the microbial oxidation of all CH₄ that passes through diffusively^{76,77}. In wetland environments, for example, methanotrophs typically oxidize 20–60% of the CH₄ produced in subsurface permafrost⁷⁸. Therefore, the most efficient routes of CH₄ dispersion into the atmosphere are ebullition and aerenchymous transference in thermokarst wetlands and lakes, ~4% of the global methane budget^{24,27,79}.

In thawed permafrost, microbial carbon transformation is impacted by soil moisture, temperature, light and nutrient availability^{54,78,80–82}. With increased inundation related to changing precipitation or abrupt thaw, CH₄ release will increase proportionally with anoxic environment expansion as microbial carbon transformation increases⁸³. In a recent example, in the tundra north of 60° latitude, subsurface CH₄ oxidation doubled (to ~5.5 TgCH₄ per year) between 2000 and 2016, indicating the potential for an increasing trend in methane release⁸⁴. However, in thawed permafrost, zones with higher redox potential create ideal regions for methanotrophs to convert CH₄ to CO₂ at a similar rapidity, making moisture and aeration essential determinants of greenhouse gas composition^{16,27,62}.



Permafrost-affected soil carbon content: kgC m⁻² (% region vulnerable to type of thawing)

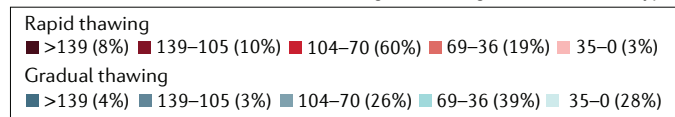


Fig. 2 | Vulnerability of carbon stocks to permafrost thaw. Permafrost regions by carbon content affected by rapid or abrupt (reds) and gradual (blues) thaw. There is noticeable overlap between areas of greatest warming (FIG. 1b) and the 20% of ice-rich regions with a potential for abrupt thaw⁴⁰. Adapted from REF.⁴⁰, Springer Nature Limited.

Small-scale processes, such as rhizome priming and nutrient availability, also impact large-scale carbon emissions trends^{17,85}. In rhizome priming, changes in the microbial respiration of organic carbon are driven by plant roots. The compounding effect of increased microbial community activity, carbon availability, and soil pH or density changes increase respiration up to 380%¹⁷. In the presence of oxygen, rhizome priming accelerates carbon decomposition up to fourfold, leading to a potential Arctic loss of about 40 PgC by 2100 from this mechanism alone. Rhizome priming can directly enable the enhanced incorporation of older carbon⁸⁶, predominantly in shallower permafrost strata, with 84% of transformation in soils shallower than 20 cm (REF.¹⁷).

Carbon emissions from permafrost-affected areas are often measured during the summer, overlooking winter emissions. However, winter carbon loss is difficult to observe or model, increasing the potential that there is an unquantified winter carbon release. In situ monitoring advances highlight an increase in microbially mediated winter carbon emissions of 73 ± 11% since 1975, potentially outpacing summer uptake capacity^{12,87}. Higher winter temperatures associated with global anthropogenic climate warming increase microbial activity and meltwater, increasing CH₄ emissions

throughout the winter¹⁴. The variability and trajectory of CH₄:CO₂ emission ratios from dynamic permafrost environments emphasize the importance of understanding the complexity of microbially mediated processes and the need to constrain the spatiotemporal heterogeneity of landscape change in the warming Arctic^{16,27,62}.

Increasing wildfire disturbances. Arctic wildfires rapidly expand the active layer of permafrost, mobilizing carbon, burning vegetation and promoting thermokarst development^{21,88,89}. Northern boreal forests store substantial carbon stocks, the loss of which could impact the PCF in the short term⁹⁰. As the climate warms, Arctic wildfires are projected to increase 130–350% by the mid-century, releasing above-ground biomass and a growing quantity of permafrost carbon, while abruptly altering the landscape²⁰. Increases in severity, frequency and extent of wildfires in boreal landscapes underlain by discontinuous permafrost and tundra landscapes with continuous permafrost can amplify permafrost degradation, simultaneously altering the topography and hydrologic flows⁹¹.

Permafrost thaw could transform some types of below-ground organic carbon into more flammable fuel for wildfires. During 2014, wildfires in Canada’s Northwest Territories released 8.62 ± 1.05 TgC to the atmosphere, with ~30% of emissions attributed to the combustion of fuels that predated the last fire and, thus, could be considered early-Holocene-aged carbon²⁰. This loss of legacy carbon during the 2014 fires represented more than 20% of the mean annual net primary productivity in global boreal forests²⁰. In 2020, over 50% of Arctic wildfires burned permafrost areas with high ice content, suggesting a substantive transformation in fuel availability⁹². Moreover, wildfires are extending beyond the traditional June–August fire season into the shoulder season months. Overwintering or ‘zombie fires’ burn year-round underground, even during the cold season^{21,92}. These smouldering, below-ground fires could release legacy carbon from environments previously thought to be fire-resistant^{21,92}, and be responsible for up to 38% of the total burned area in the Arctic⁹³.

Incorporating wildfire disturbances and its impacts on thermokarst into permafrost and PCF models is a critical, missing component of constraining projections of future Arctic carbon emissions. Though difficult, the ability to integrate changing dynamics into static permafrost system models and observations is a necessary step to improving forecasting and the detection of carbon release.

Understanding carbon across scales

As the Arctic rapidly changes, the scientific community has sought to expand its capacity to monitor, understand and predict transformation and carbon release^{60,94,95}. Instrumentation designed to sample across spatial and temporal scales has improved understanding of abrupt thaw dynamics^{26,27}, the age and impact of released carbon^{3,35,96}, the effects of changing Arctic hydrology^{63,97} and the importance of technological integration in forecasting future dynamics^{98,99}.

Detection of carbon release spans multiple scales and integrates data from multiple methodologies (TABLE 1).

Ebullition

The action of bubbling or boiling.

Aerenchymous transference

Movement of gas through air spaces found in aquatic plants.

Rhizome priming

The stimulation of microbial organic matter remineralization due to plant root activity.

Zombie fires

Fires that burn year to year and extend through the winter into the early spring, before wildfire season.

For example, land plots and flux chambers are used to quantify and characterize carbon release from specific environments at the 1–10-m scale⁷⁶. Eddy covariance (EC) towers monitor surface–atmosphere fluxes of carbon, water and energy on scales of 100–1,000 m (REF.⁶⁷). At regional to continental levels, tall tower networks complemented by larger-scale aircraft campaigns deliver carbon release information on 10–1,000-km scales¹⁰⁰. For observation scales >1,000 m, a growing number of satellite sensors monitor surface and atmospheric variables that can be used to infer carbon flux across the entire Arctic^{101–103}. This combination of observations and model scenarios across scales provides a picture of rapid thaw and an abrupt loss of carbon (FIG. 2), on the order of decades or less.

Laboratory-based research. Laboratory-based research (usually on samples collected in the field) has produced important information on the dynamics of permafrost microbial communities, including the myriad survival strategies that have preserved extremophile permafrost microbes for up to a million years in stasis. These adaptations include the production of carotenoids¹⁰⁴, high abundance of stress-response genes¹⁰⁵, lipid-rich membrane fluidity¹⁰⁶, dormancy^{105,107} and DNA repair^{108,109}.

DNA-based analyses, including metagenomics and 16S rRNA gene sequencing, have illuminated adaptations, origins, metabolic potential and microbial community composition in representative permafrost samples^{70,110,111}. However, these analyses do not distinguish between live

and dead cells, which is critical to determining the carbon transformation potential of microorganisms¹¹². Therefore, advances in live–dead staining and endospore enrichment with conditions controlling for pH, acidity and carbon concentration are increasingly critical to determine the carbon transformation potential of permafrost microbial communities^{112–114}.

Incubation of permafrost and permafrost-affected soil samples is another method used to understand microbially mediated carbon release. Carbon release was 3.4 times higher in aerobic conditions than in anaerobic conditions in permafrost incubations¹¹⁵. A greater loss of permafrost carbon is, therefore, predicted for oxic conditions by laboratory assessments and modelling. However, as this loss is expected to be primarily in the form of CO₂ emissions, an equal amount of released CH₄ under anaerobic conditions has considerably more warming potential⁶⁰. The increase in activity from reactivated microorganisms in anoxic conditions could increase carbon emissions across the Arctic by 27–38 TgCH₄ per year by 2100, effectively doubling current CH₄ emissions⁸⁵. Therefore, determining the processes driving the degradation and release of permafrost carbon by the increased microbial activity expected with permafrost thaw is essential to understanding the transformation of permafrost carbon.

In situ and fieldwork. In situ research is critical to accurately upscaling projected changes to permafrost ecosystems^{116–118}, by providing the data continuity needed

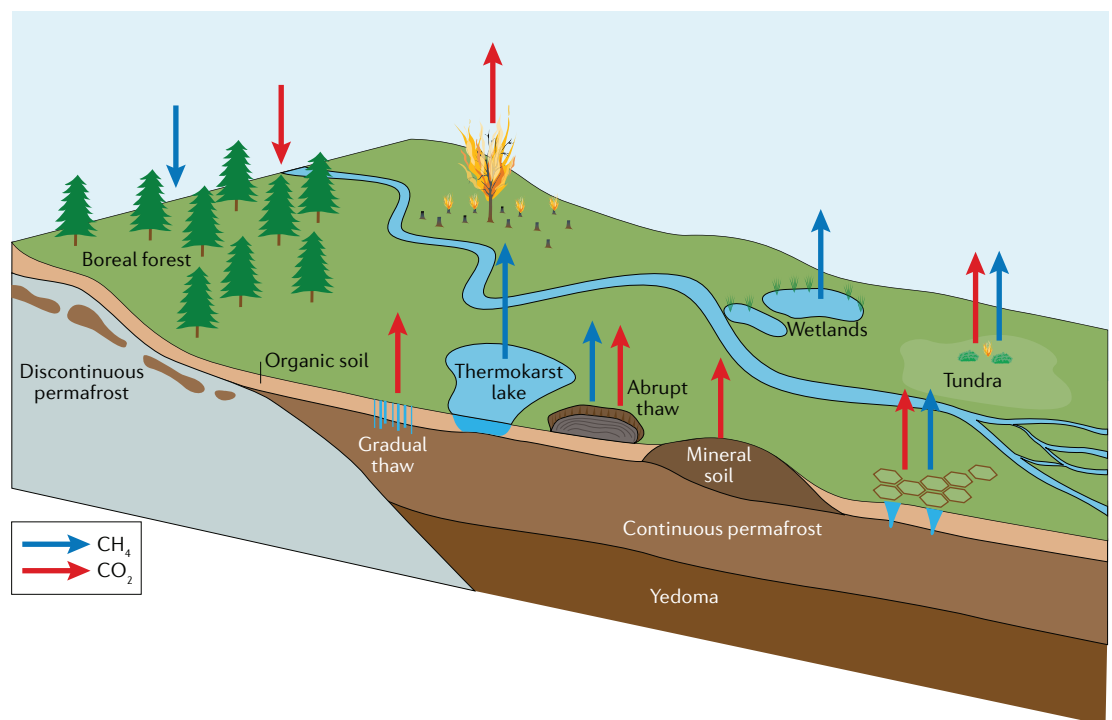


Fig. 3 | Carbon flux dynamics in permafrost landscapes. Carbon transformation in an idealized Arctic environment experiencing wildfire and thermokarst disturbances. Sources and sinks for CO₂ and CH₄ are indicated by arrows. Tundra has lost an estimated 761.8 gC m⁻² since ~2005. Currently, thermokarst thaw lakes emit ~14–18 TgC per year. Overall, permafrost-affected regions in the Arctic are trending towards greater carbon release; wildfires in boreal forests could increase 130–560% by 2100 and carbon release from abrupt thaw is projected to increase to 613–802 TgCO₂e per year. Adapted with permission from REF.¹⁹⁵, ACIA 2004.

Table 1 | The range and availability of observational data sources for Arctic greenhouse gas assessments

Observation technique	Resolution	Arctic coverage	Timescale	Locations	Advantages (+) and disadvantages (-)	Example missions or programmes
In situ						
Permanent	Point measurements	Local coverage	Multi-year data sets	Dozens to hundreds, on a (semi-) permanent basis	+ Long-term data sets that are able to identify trends – Highly localized data with few locations; not a coherent network	NOAA Earth System Research Laboratories Global Monitoring Laboratory
Campaign	Point measurements	Local coverage	Several hours or days	Variable	+ Can target locations not available from other data sets – Expensive; short-term trends, usually not in winter	The Multidisciplinary drifting Observatory for the Study of Arctic Climate (MOSAIC)
Towers	Point measurements in the boundary layer (>50 m)	100–1,000 m	Multi-year data sets	Dozens to hundreds, on a (semi-) permanent basis	+ Identifies transport of trace gases in the boundary layer – Poor coverage, few permanent locations, limited sensitivity, not a coherent network	FLUXNET
Airborne						
In situ	Point measurements in the troposphere	Regional coverage (profiles)	Several hours or days	Variable, depending on study Typically focused to specific areas and times	+ Bridges spatial scales between local and satellite data – Expensive to run regular campaigns	HIAPER Pole-to-Pole Observations (HIPPO) of Carbon Cycle and Greenhouse Gases Study
Remote sensing (active and passive)	Surface pixels (>25 m)	Regional coverage	Several hours or days	Variable, depending on study Typically focused to specific areas and times	+ Bridges gaps between scales; good for satellite validation and targeted observations – Expensive to run regular campaigns	Airborne Visible-Infrared Imaging Spectrometer – Next Generation (AVIRIS-NG)
Satellite						
Short-wave infrared	Surface pixels (>5.5 × 7 km CH ₄ ; >1 × 2 km CO ₂)	Seasonal daylight coverage	Multi-year data sets	Low Earth orbit, giving global daily coverage Geostationary orbit, giving hourly coverage of localized regions	+ Daily coverage of the Arctic CH ₄ – Large spatial footprints, poor coverage in winter months, CO ₂ observations are limited by satellite swath	GOSAT ¹⁷⁸ , OCO-2 (REF. ¹⁷⁹), TanSat ¹⁸⁰ , GOSAT-2 (REF. ¹⁸¹), Sentinel-5P ¹⁸² , GHGSat, MERLIN ^{183,184} , CO2M ¹⁸⁵ , Sentinel-5 (REF. ¹⁸⁶), AIM-North ¹⁸⁷ , geoCARB ¹⁸⁸
Thermal infrared	Pixels (2 × 2 km)	Total coverage	Multi-year data sets	Low Earth orbit, giving global daily coverage, or geostationary orbit, giving hourly coverage of localized regions	+ Daily coverage of the Arctic, sensitive to the troposphere – Low sensitivity to the surface, large spatial footprint	Aqua/AIRS ¹⁸⁹ , MetOp-IASI ¹⁹⁰ and Suomi NPP CrIS ^{191,192}

to understand the local dynamics of permafrost thaw. Analyses of gradual thaw have now spanned multiple decades, documenting the release and uptake of carbon at the site to landscape scales, often using rivers or lakes as landscape integrators¹¹⁹. For example, one of the longest in situ assessments of carbon exchange in Alaskan tundra and rivers systems identified a local increase in carbon emission and uptake over the last 15 years, with a net carbon loss of 781.6 gC m⁻² (REFS^{120,121}). This increase suggests that, although Arctic vegetation increases could lead to higher carbon uptake^{7,122}, an increase in respiration could offset these gains.

In situ monitoring is also necessary in identifying soil-level changes that are difficult or impossible to

monitor using remote sensing tools. For example, in situ soil temperature profile measurements have shown that active layer zones at 20–30-cm depths in tundra wetlands remain thawed, but hovering near 0 °C for months into the cold season. This so-called zero curtain period extends microbial metabolism and both CO₂ and CH₄ emissions well past the point when the surface has refrozen^{12,14,87}. The shoulder season period currently contributes an estimated ~50% of annual permafrost wetland CH₄ emissions^{14,87}. Similarly, a synthesis of northern thermokarst lake emissions suggested that Arctic lakes and ponds could increase CH₄ release 20–54% before 2100, as warm seasons lengthen with climate change⁷⁴.

Zero curtain

The transition of water to ice is slowed due to latent heat release in the surrounding soil, despite sub-zero air temperatures.

Year-over-year permafrost changes are more visible where thaw meets physical erosion, making fieldwork especially valuable. In an Alaskan riverbank, for example, retrieved data covering 1995–2011 illustrates permafrost retreat of ~11 m per year (880 tons of C)¹²³. As permafrost thaw increases hydrologic change, these dynamics might be mirrored across increasingly large areas. While in situ data are not immediately able to be upscaled, long-term laboratory and field research provide invaluable information on permafrost loss and carbon transformation, especially in combination with remote sensing tools.

Flux towers. Measurements from EC flux towers span the gap between in situ terrain-scale research and airborne sensing at the landscape level. Across the Arctic, over 212 active flux towers¹²⁴ have revealed carbon flux patterns and storage, and physical or seasonal controls on emission¹²⁵. Flux towers can incorporate vertical surface and near-atmosphere-level fluxes to quantify photosynthesis, evapotranspiration, soil moisture and respiration^{125,126}. Placement versatility has further highlighted carbon fluxes from lake and thermokarst environments. For example, when placed in lakes, flux towers expose winter ebullition and summer uptake patterns, incorporating atmospheric pressure and temperature dynamics¹²⁷. Flux towers are often able to span the gap between in situ and atmospheric measurements, providing critical information about fluxes in the near-surface atmosphere.

When incorporated into systems models, flux tower data are instrumental in constraining model outputs. Utilizing flux tower data in carbon models resulted in a 13.4% decrease in mean carbon residence for tundra ecosystems in Alaska, indicating that carbon cycling in the boreal ecosystem could be increasing⁶⁵. The granular, scalable data provided by flux towers identify ecosystem controls that are difficult to model and measure.

Advances in instrument and analysis techniques have enabled the application of airborne EC flux measurements to evaluate regional-scale carbon release in the Arctic^{128,129}. Airborne EC fluxes provide a powerful tool with which to test methods for upscaling flux tower measurements to regional scales^{130–132}, as well as regional-scale inversions of atmospheric concentration data from tall towers and/or aircraft^{12,133–136}. Pan-Arctic CO₂ and CH₄ flux measurements could soon be possible by integrating current and future space-based flux towers by matching plot-scale measurements under known conditions¹²⁵.

Remote sensing. Satellite observations are expanding the variety and quality of global data available to researchers, providing an unprecedented view of carbon cycle dynamics and PCF processes. High-resolution remote sensing tools retrieve data on greenhouse gases with high spatial resolution and low noise interference, determining CO₂ and CH₄ hotspots¹³⁷. Current on-orbit satellite spectrometers that gather CO₂ or CH₄ measurements at high latitudes provide diverse data (TABLE 1). Satellites show high potential for categorizing soil carbon^{10,138}, upscaling emissions²⁴ and identifying land surface heterogeneity at high latitudes¹⁹. Soil wetting and carbon

content have been quantified with multispectral^{19,139} and synthetic aperture radar observations¹⁴⁰. An increase of data on heterogeneous Arctic landscapes is already improving methane hotspot detection at specific sites, allowing further exploration of localized emission across wetlands, thermokarst and tundra¹⁰⁰. The high-resolution observations from satellite hyperspectral instruments could be vital to determining hydrologic heterogeneity and land cover change^{19,24}. However, remote sensing for jointly mapping carbon hotspots and permafrost thaw is still in its infancy⁹⁹.

At an international level, the combined efforts of numerous satellites are ideal for integrating all existing data, as missions from ESA, NASA and others work to standardize data for rapid sharing and transposition. Future satellite missions are expected to improve seasonal and diurnal observations (TABLE 1). For example, MERLIN (launch ~2025) will measure atmospheric methane independent of sunlight, seasonality or some cloud cover. Satellite CO2M (launch 2025) will measure CO₂ and CH₄ total columns to increase carbon flux monitoring at small pixel sizes (2 × 2 km) and a relatively wide field of view (250 km). Smaller pixel sizes will improve cloud-free observations, enabling scale-matching between satellite data, aircraft remote sensing, flux towers and in situ sampling. Airborne remote sensing of Arctic methane hotspots using hyperspectral imagery with metre-scale pixels indicates that upcoming space-based hyperspectral imagers (such as EnMAP, PRISMA-SG, SBG and CHIME) will make major contributions to the understanding of Arctic carbon emissions¹⁰⁰. The potential of these imagers is foreshadowed by the use of Sentinel-2 data (20-m resolution) to detect methane point sources¹⁴¹.

While remote sensing is practical on a global scale, higher-spatial-resolution data (below 20 m) is required to consistently determine precise carbon release locations. Satellite carbon flux estimates are limited in summer by low reflectivity from ice, snow and water, and are severely degraded during the Arctic night (October–April). Furthermore, thermal infrared satellite sensitivity is largest in the upper troposphere between 200 and 750 hPa, making it challenging to identify specific release locations at the surface. Comparing satellite data to in situ carbon flux and land change measurements requires high-efficacy downscaling tools that are still under development. Similarly, interpolating data from flux towers with footprints typically ranging from 0.01 to 1.0 km² for regional or pan-Arctic carbon fluxes requires accurate upscaling capabilities¹⁴². The diverse scales, modelling parameterizations and locational data mean that upscaling does not match downscaling¹⁴³. The discontinuity between flux data across available instruments makes estimating and predicting Arctic carbon release difficult^{144,145}.

Modelling. Despite the advances in measuring and monitoring permafrost carbon dynamics, efforts to model Arctic changes lag. However, some notable progress has been made. In the past 10 years, models have produced the first reliable forecasts of permafrost carbon release. Based the RCP4.5 and RCP8.5 scenarios, 15 model

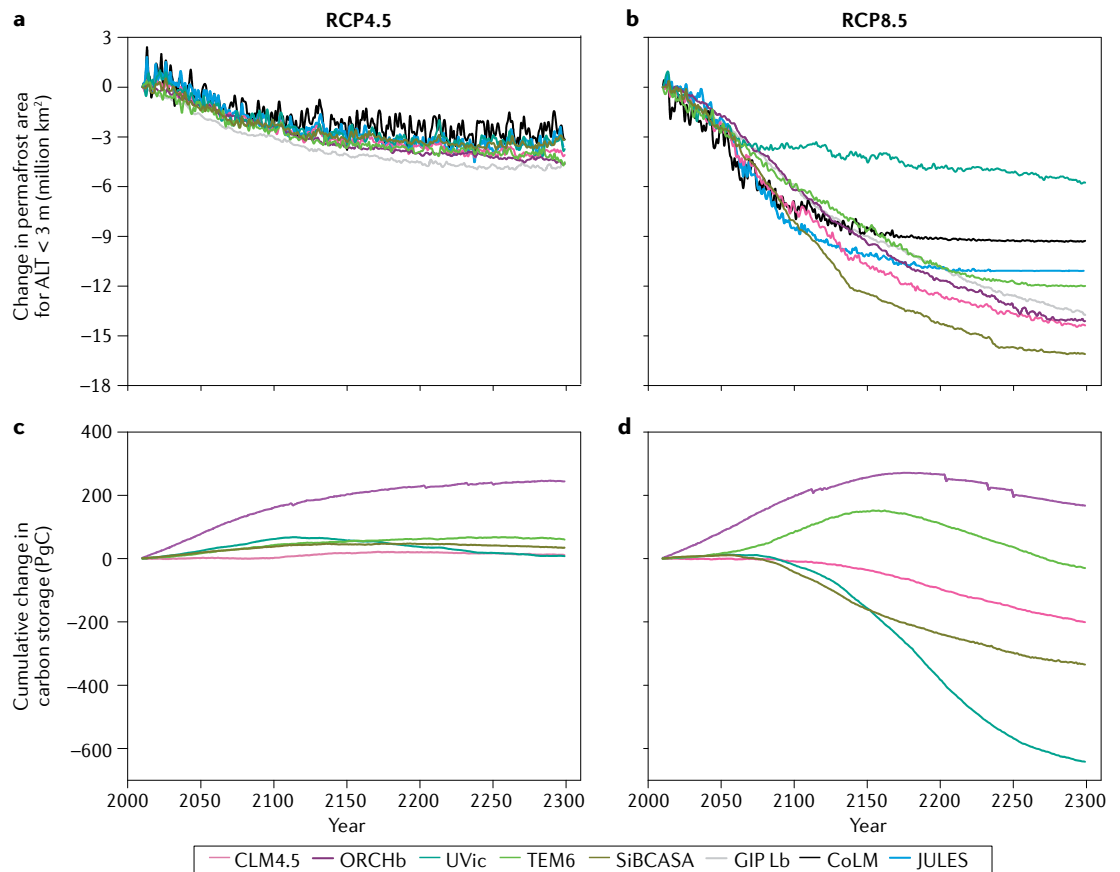


Fig. 4 | Simulated cumulative changes in permafrost area and storage capacity. **a** | Projected permafrost active layer thickness (ALT) less than 3 m over 2010–2299 in several models forced with RCP4.5. **b** | As in panel **a** but for RCP8.5. **c** | Predicted total ecosystem carbon storage over 2010–2299 under RCP4.5. **d** | As in panel **c** but for RCP8.5. Vegetation growth under RCP scenarios might be a primary source of carbon uptake over the next 100 years, as the Arctic shifts towards a new steady state. Adapted with permission from REF.⁷, PNAS.

simulations all predicted a total loss of near-surface permafrost (less than 3 m deep) over the region by 2100, with differences in the magnitude of loss rates among the models (0.2 to $58.8 \times 10^3 \text{ km}^2$ per year)⁷ (FIG. 4). The simulations indicated a total loss of 3 to 5 million km² permafrost (mean loss 4 PgC) in the RCP4.5 scenario and 6 to 16 million km² (mean loss 341 PgC) for the RCP8.5 scenario. An increase in future net primary productivity is modelled to increase vegetative carbon storage from 156 to 954 TgC per year between 2010 and 2299. However, the modelled vegetation carbon gains were not substantial enough to compensate for even larger soil carbon losses under RCP8.5, the current Arctic trajectory⁷. The magnitude of this offset is limited by temperature and nutrients, with wide variation in models projecting CO₂ plant uptake^{7,89,146,147} (FIG. 5).

Similarly, models focusing on small-scale permafrost processes forecast an increase of ~12 times current carbon release by 2100 under RCP8.5 (REF.⁶⁴). Deepening active layer thaw estimates for this period ranged from one to eight times deeper relative to 2020, even without considering ground subsidence in regions with high ice content⁶⁴. As models are refined, patterns of abrupt thaw emerge more strongly, impacting soil temperature, soil moisture conditions, surface fluxes and vegetation^{148,149}.

To truly capture Arctic thaw dynamics, system models must integrate scaled data between land surface observations and terrain-level permafrost models^{149–152}. Since carbon partitioning depends on numerous environmental factors, iterative system models incorporating vegetation sensitivity, the physical dynamics driving permafrost degradation, hydrologic cycling and microbial transformation must all be included^{16,72,76}. Whether and to what extent the permafrost landscape, already interspersed with thaw lakes and thermokarst, transforms from a carbon sink into a carbon source in a warmer world can only be answered with combined modelling and observational data⁴⁰.

Summary and future perspectives

The Arctic is warming two to four times faster than the global average, changing thaw dynamics, vegetation type and density. Yet, it remains one of the Earth's least investigated regions¹⁵³, challenging forecasts for future dynamics. Despite these challenges, advances in modelling and forecasting thaw dynamics has led to a better understanding of carbon release and landscape change^{3,55}. In situ and satellite observations dedicated to monitoring the carbon system have generated an entirely new data set for the research community^{103,154}.

These observations are being bridged by airborne campaigns that provide new, seasonal data across the Arctic^{100,155}. Scientific cooperation across diverse fields has already increased the modelling accuracy and data integration for carbon transport, permafrost thaw and climate scenarios^{7,153}. However, further international collaboration, monitoring and exploration is needed to determine the areas of greatest change. All efforts to quantify carbon release expand scientific understanding of complex, changing and emergent dynamics of a warming Arctic. Topics that have the greatest potential to transform abilities to monitor or forecast permafrost carbon emissions, and, thereby, understand future tipping points in the climate crisis, are now discussed.

Systematically monitor carbon mobilization. A comprehensive synthesis of Arctic carbon fluxes concluded that the Arctic has been a sink for carbon for decades, but the strength of this sink is uncertain¹⁵⁶. Contemporary estimates suggest a sink of 110 TgC per year CO₂ (range 80–291 TgC per year) and emission of 19 TgC per year CH₄ (range 8–29 TgC per year)¹⁵⁶. The high level of uncertainty highlights that the current atmospheric CO₂ and CH₄ measurement system is inadequate to

quantify the Arctic carbon budget, identify the source(s) of changes in long-term atmospheric trends and detect the onset of large-scale old carbon mobilization from permafrost, a critical Arctic tipping point^{157–159} (FIG. 5).

A new, unified observing system tailored to monitoring the PCF is urgently needed. A dense network of tall towers, airborne vertical profile measurements and flux towers should be deployed and maintained through the coming decades. The resulting multi-decadal time series will serve as the foundation of the observation system. Rapid development and deployment of active CO₂ and CH₄ remote sensing tools are required to supplement the growing collection of passive, space-based remote sensing instruments, which are challenged by the polar night¹⁵¹. Regular, sustained deployment (at intervals of less than a decade between launches) of active CO₂ and CH₄ sensors should be investigated as a potential method for obtaining these data in a cost-effective way, and on an accelerated schedule compared with airborne and space-based systems. Finally, the observational network should be augmented with radiocarbon analyses of dissolved carbon to monitor changes in the old carbon fraction mobilizing in the Arctic^{26,41}. Emergent optical methods^{160,161} could soon offer continuous in situ detection of atmospheric ¹⁴CO₂ and ¹⁴CH₄ to complement the traditional mass spectral analyses of whole air samples¹⁶². These observations will be essential to identifying where and when large amounts of old carbon begin to mobilize.

Refine Arctic hydrology in large-scale models. Debate continues on the future hydrologic state of the Arctic. Whether climate shifts will force the Arctic towards overall drying or wetting could have lasting implications for carbon. In a greener, wetter Arctic, plants will offset some or all permafrost carbon emissions through plant uptake and the incorporation of detritus in soils^{7,163}. However, in a browner, drier Arctic, respiration and, therefore, CO₂ emissions from decomposing soils are expected to increase, while the amount and flammability of fuels for wildfires grow^{80,91,92,164}. Currently, Arctic climate models contain substantial uncertainty in precipitation, evapotranspiration and runoff parameters, making it challenging to forecast coupled changes in hydrology and vegetation⁹⁷. Moreover, the complex changes in hydrologic flow, topography and vegetation associated with abrupt thaw are not currently being simulated in large-scale models. The development of physically based hydrological models that include key cold region processes such as ground freeze/thaw state will be key in simulating the impacts of permafrost thaw on complex patterns of vegetation and hydrological change¹⁶⁵, which, ultimately, will lead to improved estimates of the PCF.

Represent permafrost processes in ESMs. Accurately projecting the timing and magnitude of the PCF has hindered the oversimplification of permafrost dynamics in many ESMs^{3,166}. Greater collaboration across observational and modelling disciplines are needed to remedy this oversimplification. Additionally, ESMs continue to neglect or minimize the impact of Arctic cold season

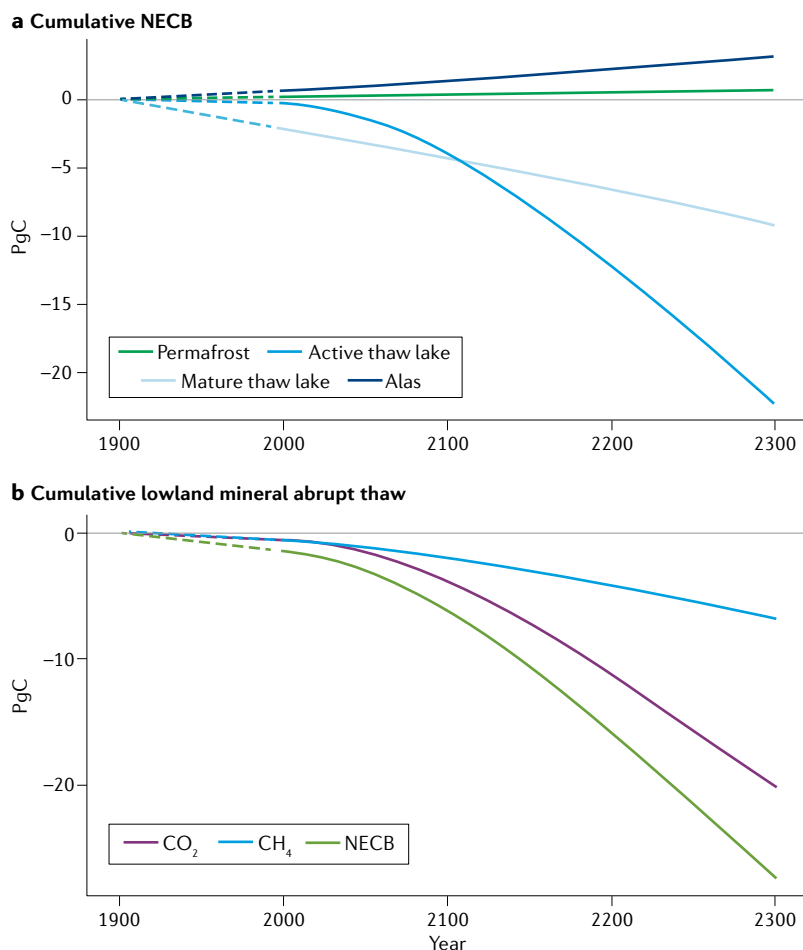


Fig. 5 | Projected change in Arctic net carbon balance to 2300. **a** | Cumulative net ecosystem carbon balance (NECB) for different environments. **b** | Partitioning of carbon into CO₂ and CH₄. A decreasing trend in overall ecosystem carbon balance is apparent until the year 2300 for thaw lakes, with a slight increase in carbon balance in permafrost. Adapted from REF.³, Springer Nature Limited.

processes and winter CH₄ emissions on annual carbon budgets¹⁶⁷. The occurrence of notable winter CO₂ fluxes has been known since at least the 1960s¹⁶⁸, yet, models still do not simulate cold season fluxes accurately.

Forecasting drivers of permafrost thaw — shoulder season length, precipitation and warming rates — continues to present challenges. Seasonal changes can be captured with satellite observations but are often confined to coarse resolution (tens of kilometres), which does not reflect the heterogeneity of Arctic landscapes^{83,169}. Therefore, estimates of winter carbon flux vary greatly, from 0.19 to 210 gCO₂-C m⁻² per year, with uncertainty driven by observational challenges, and require ground-based validation¹⁷⁰. While snow has long been recognized as one of the most important controls on permafrost resilience to thaw, cold season carbon emissions are more important to annual emissions than previously thought^{14,87,171}. Future research should minimize uncertainties surrounding the estimation of seasonal thaw and year-round soil respiration through ongoing remote sensing and in situ validation^{7,40}. Collaborative, international teams will be required to provide the continuity and quality of data sought.

Improve understanding of vegetation and carbon dynamics. Arctic greening is projected to offset at least a portion of permafrost carbon release through biomass formation and the incorporation of plant detritus in soils^{7,163}. Under the RCP4.5 scenario, gradual thaw model simulations suggest that vegetative carbon storage could increase from 156 to 954 TgC per year by 2100, offsetting permafrost carbon emissions⁷.

Large-scale ESMS must be diverse enough to capture both large variation in simulated Arctic CO₂ plant uptake^{7,89,146,147} and ecosystem carbon balance often dictated by the strength of plant CO₂ fertilization in combination with vegetation response to climate^{7,172}. For example, permafrost thaw lakes could serve an essential carbon sequestration function, with vegetation and sediment storing up to 47 ± 10 gC m⁻² per year¹⁷³. However, thermokarst lake sequestration relies on

permafrost stability, the loss of which leads to drainage and the release of carbon¹⁷³. A better understanding of how to incorporate carbon release with abrupt thaw into ESMS, plus a more realistic simulation of changing plant distributions and uptake potential, represent important topics for future research concerning both gradual and abrupt thaw.

Understand palaeo-permafrost for insight into future change. Little is known about how the modern destabilization of permafrost compares with past periods of abrupt climate change. Permafrost thaw rates were rapid during the early Holocene, at least for thermokarst lakes¹⁷³, but probably occurred under a lower temperature threshold than they do now, as the rapid warming of the past 100 years outpaces much of the Holocene. Similarly, a punctuated pulse of permafrost carbon released to the atmosphere at the end of the Last Glacial Maximum might have driven the global temperature increase recorded at the start of the interglacial^{174,175}. Research incorporating extremophiles preserved in permafrost, carbon dating and nutrient characterization should be prioritized as permafrost microbes increasingly enter the modern ecosystem.

Improve data scaling. Losses of old carbon through permafrost thaw, particularly via abrupt thaw features such as thermokarst lakes, are typically described and upscaled as hotspots¹⁷⁶. Future research should focus on the point-source and atmosphere flux data required to frame permafrost thaw carbon emissions within an ecosystem control point framework¹⁷⁷, which will lead to a more robust mechanistic understanding of permafrost biogeochemistry and improved ability to scale and simulate the spatiotemporal dynamics of the PCF. Coordination across field, airborne and remote sensing campaigns is essential to the success of observing carbon emissions across scales, enabling better predictions for the future of the Arctic.

Published online 11 January 2022

- Olefeldt, D. et al. Circumpolar distribution and carbon storage of thermokarst landscapes. *Nat. Commun.* **7**, 13043 (2016).
- Lindgren, A., Hugelius, G. & Kuhry, P. Extensive loss of past permafrost carbon but a net accumulation into present-day soils. *Nature* **560**, 219–222 (2018).
- Turetsky, M. R. et al. Carbon release through abrupt permafrost thaw. *Nat. Geosci.* **13**, 138–143 (2020).
- Walter Anthony, K. et al. Methane emissions proportional to permafrost carbon thawed in Arctic lakes since the 1950s. *Nat. Geosci.* **9**, 679–682 (2016).
- Schuur, E. A. G. et al. Climate change and the permafrost carbon feedback. *Nature* **520**, 171–179 (2015).
- Gasser, T. et al. Path-dependent reductions in CO₂ emission budgets caused by permafrost carbon release. *Nat. Geosci.* **11**, 830–835 (2018).
- McGuire, A. D. et al. Dependence of the evolution of carbon dynamics in the northern permafrost region on the trajectory of climate change. *Proc. Natl Acad. Sci. USA* **115**, 3882–3887 (2018).
- Heffernan, L., Estop-Aragones, C., Knorr, K. H., Talbot, J. & Olefeldt, D. Long-term impacts of permafrost thaw on carbon storage in peatlands: deep losses offset by surficial accumulation. *J. Geophys. Res. Biogeosci.* **125**, e2019JG005501 (2020).
- Chadburn, S. E. et al. An observation-based constraint on permafrost loss as a function of global warming. *Nat. Clim. Chang.* **7**, 340–344 (2017).
- Bartsch, A. et al. Can C-band synthetic aperture radar be used to estimate soil organic carbon storage in tundra? *Biogeosciences* **13**, 5453–5470 (2016).
- Obu, J. et al. Northern Hemisphere permafrost map based on TTOP modelling for 2000–2016 at 1 km² scale. *Earth Sci. Rev.* **193**, 299–316 (2019).
- Commane, R. et al. Carbon dioxide sources from Alaska driven by increasing early winter respiration from Arctic tundra. *Proc. Natl Acad. Sci. USA* **114**, 5361–5366 (2017).
- Natali, S. M. et al. Permafrost carbon feedbacks threaten global climate goals. *Proc. Natl. Acad. Sci. USA* **118**, e2100163118 (2021).
- Zona, D. et al. Cold season emissions dominate the Arctic tundra methane budget. *Proc. Natl Acad. Sci. USA* **113**, 40–45 (2016).
- Comyn-Platt, E. et al. Carbon budgets for 1.5 and 2 °C targets lowered by natural wetland and permafrost feedbacks. *Nat. Geosci.* **11**, 568–573 (2018).
- Heslop, J. K. K. et al. A synthesis of methane dynamics in thermokarst lake environments. *Earth Sci. Rev.* **210**, 103365 (2020).
- Keuper, F. et al. Carbon loss from northern circumpolar permafrost soils amplified by rhizosphere priming. *Nat. Geosci.* **13**, 560–565 (2020).
- Nitze, I., Grosse, G., Jones, B. M., Romanovsky, V. E. & Boike, J. Remote sensing quantifies widespread abundance of permafrost region disturbances across the Arctic and Subarctic. *Nat. Commun.* **9**, 5423 (2018).
- Lara, M. J. et al. Local-scale Arctic tundra heterogeneity affects regional-scale carbon dynamics. *Nat. Commun.* **11**, 4925 (2020).
- Walker, X. J. et al. Increasing wildfires threaten historic carbon sink of boreal forest soils. *Nature* **572**, 520–523 (2019).
- Rey, D. M. et al. Wildfire-initiated talik development exceeds current thaw projections: observations and models from Alaska's continuous permafrost zone. *Geophys. Res. Lett.* **47**, e2020GL087565 (2020).
- Kim, J. S., Kug, J. S., Jeong, S. J., Park, H. & Schaeppman-Strub, G. Extensive fires in southeastern Siberian permafrost linked to preceding Arctic Oscillation. *Sci. Adv.* **6**, eaax3308 (2020).
- Vonk, J. E., Tank, S. E. & Walvoord, M. A. Integrating hydrology and biogeochemistry across frozen landscapes. *Nat. Commun.* **10**, 5377 (2019).
- Saunio, M. et al. The global methane budget 2000–2017. *Earth Syst. Sci. Data* **12**, 1561–1623 (2020).
- Williams, J. W., Ordóñez, A. & Svenning, J. C. A unifying framework for studying and managing climate-driven rates of ecological change. *Nat. Ecol. Evol.* **5**, 17–26 (2021).

26. Schwab, M. S. et al. An abrupt aging of dissolved organic carbon in large Arctic rivers. *Geophys. Res. Lett.* **47**, e2020GL088823 (2020).
27. Walter Anthony, K. M. et al. Decadal-scale hotspot methane ebullition within lakes following abrupt permafrost thaw. *Environ. Res. Lett.* **16**, 35010 (2021).
28. Goldstein, A. et al. Protecting irrecoverable carbon in Earth's ecosystems. *Nat. Clim. Chang.* **10**, 287–295 (2020).
29. Turner, M. G. et al. Climate change, ecosystems and abrupt change: science priorities. *Phil. Trans. R. Soc. B* **375**, 20190105 (2020).
30. Fountain, A. G. et al. The disappearing cryosphere: impacts and ecosystem responses to rapid cryosphere loss. *Bioscience* **62**, 405–415 (2012).
31. Gruber, S. Derivation and analysis of a high-resolution estimate of global permafrost zonation. *Cryosphere* **6**, 221–233 (2012).
32. Zou, D. et al. A new map of permafrost distribution on the Tibetan Plateau. *Cryosphere* **11**, 2527–2542 (2012).
33. Sayedi, S. S. et al. Subsea permafrost carbon stocks and climate change sensitivity estimated by expert assessment. *Environ. Res. Lett.* **15**, 124075 (2020).
34. Smith, S. L., O'Neill, H. B., Isaksen, K., Noetzli, J. & Romanovsky, V. E. The changing thermal state of permafrost. *Nat. Rev. Earth Environ.* <https://doi.org/10.1038/s43017-021-00240-1> (2022).
35. Strauss, J. et al. Deep Yedoma permafrost: a synthesis of depositional characteristics and carbon vulnerability. *Earth Sci. Rev.* **172**, 75–86 (2017).
36. Strauss, J. et al. The deep permafrost carbon pool of the Yedoma region in Siberia and Alaska. *Geophys. Res. Lett.* **40**, 6165–6170 (2013).
37. Elder, C. D. et al. Greenhouse gas emissions from diverse Arctic Alaskan lakes are dominated by young carbon. *Nat. Clim. Chang.* **8**, 166–171 (2018).
38. Martens, J. et al. Remobilization of old permafrost carbon to Chukchi Sea sediments during the end of the last deglaciation. *Glob. Biogeochem. Cycles* **33**, 2–14 (2019).
39. Vonk, J. E. et al. Reviews and syntheses: effects of permafrost thaw on Arctic aquatic ecosystems. *Biogeosciences* **12**, 7129–7167 (2015).
40. Turetsky, M. R. et al. Permafrost collapse is accelerating carbon release. *Nature* **569**, 32–24 (2019).
41. Wild, B. et al. Rivers across the Siberian Arctic unearth the patterns of carbon release from thawing permafrost. *Proc. Natl Acad. Sci. USA* **116**, 10280–10285 (2019).
42. Mishra, U. et al. Spatial heterogeneity and environmental predictors of permafrost region soil organic carbon stocks. *Sci. Adv.* **7**, 5236–5260 (2021).
43. Treat, C. C. et al. Tundra landscape heterogeneity, not interannual variability, controls the decadal regional carbon balance in the Western Russian Arctic. *Glob. Chang. Biol.* **24**, 5188–5204 (2018).
44. Siewert, M. B., Lantuit, H., Richter, A. & Hugelius, G. Permafrost causes unique fine-scale spatial variability across tundra soils. *Glob. Biogeochem. Cycles* **35**, e2020GB006659 (2021).
45. Niittynen, P. et al. Fine-scale tundra vegetation patterns are strongly related to winter thermal conditions. *Nat. Clim. Chang.* **10**, 1143–1148 (2020).
46. Hope, C. & Schaefer, K. Economic impacts of carbon dioxide and methane released from thawing permafrost. *Nat. Clim. Chang.* **6**, 56–59 (2016).
47. Farquharson, L. M. et al. Climate change drives widespread and rapid thermokarst development in very cold permafrost in the Canadian High Arctic. *Geophys. Res. Lett.* **46**, 6681–6689 (2019).
48. Biskaborn, B. K. et al. Permafrost is warming at a global scale. *Nat. Commun.* **10**, 264 (2019).
49. Hood, E., Battin, T. J., Fellman, J., O'Neel, S. & Spencer, R. G. M. Storage and release of organic carbon from glaciers and ice sheets. *Nat. Geosci.* **8**, 91–96 (2015).
50. Tanski, G. et al. Rapid CO₂ release from eroding permafrost in seawater. *Geophys. Res. Lett.* **46**, 11244–11252 (2019).
51. Liljedahl, A. K., Gadeke, A., O'Neel, S., Gatesman, T. A. & Douglas, T. A. Glacierized headwater streams as aquifer recharge corridors, subarctic Alaska. *Geophys. Res. Lett.* **44**, 6876–6885 (2017).
52. Yumashev, D. et al. Climate policy implications of nonlinear decline of Arctic land permafrost and other cryosphere elements. *Nat. Commun.* **10**, 1900 (2019).
53. Woodcroft, B. J. et al. Genome-centric view of carbon processing in thawing permafrost. *Nature* **560**, 49–54 (2018).
54. Nauta, A. L. et al. Permafrost collapse after shrub removal shifts tundra ecosystem to a methane source. *Nat. Clim. Chang.* **5**, 67–70 (2015).
55. Anthony, K. W. et al. 21st-century modeled permafrost carbon emissions accelerated by abrupt thaw beneath lakes. *Nat. Commun.* **9**, 3262 (2018).
56. Hugelius, G. et al. Large stocks of peatland carbon and nitrogen are vulnerable to permafrost thaw. *Proc. Natl Acad. Sci. USA* **117**, 201916387 (2020).
57. Christensen, T. R., Arora, V. K., Gauss, M., Höglund-Isaksson, L. & Parmentier, F. J. W. Tracing the climate signal: mitigation of anthropogenic methane emissions can outweigh a large Arctic natural emission increase. *Sci. Rep.* **9**, 1146 (2019).
58. United Nations Framework Convention on Climate Change. Total aggregate greenhouse gas emissions of individual nations, annex 1. *World Resources Institute* <https://www.wri.org/resources/data-sets/climate-watch-cait-unfccc-annex-i-ghg-emissions-data> (2008).
59. Lewkowicz, A. G. & Way, R. G. Extremes of summer climate trigger thousands of thermokarst landslides in a High Arctic environment. *Nat. Commun.* **10**, 1329 (2019).
60. Knoblauch, C., Beer, C., Liebner, S., Grigoriev, M. N. & Pfeiffer, E. M. Methane production as key to the greenhouse gas budget of thawing permafrost. *Nat. Clim. Chang.* **8**, 309–312 (2018).
61. Jones, B. M. et al. Lake and drained lake basin systems in lowland permafrost regions. *Nat. Rev. Earth Environ.* <https://doi.org/10.1038/s43017-021-00238-9> (2022).
62. Matthews, E., Johnson, M. S., Genovese, V., Du, J. & Bastviken, D. Methane emission from high latitude lakes: methane-centric lake classification and satellite-driven annual cycle of emissions. *Sci. Rep.* **10**, 12465 (2020).
63. Lamontagne-Hallé, P., McKenzie, J. M., Kurylyk, B. L. & Zipper, S. C. Changing groundwater discharge dynamics in permafrost regions. *Environ. Res. Lett.* **13**, 084017 (2018).
64. Nitzbon, J. et al. Fast response of cold ice-rich permafrost in northeast Siberia to a warming climate. *Nat. Commun.* **11**, 2201 (2020).
65. Jeong, S. J. et al. Accelerating rates of Arctic carbon cycling revealed by long-term atmospheric CO₂ measurements. *Sci. Adv.* **4**, eaao1167 (2018).
66. Disher, B. S., Connor, R. F., Haynes, K. M., Hopkinson, C. & Quinton, W. L. The hydrology of treed wetlands in thawing discontinuous permafrost regions. *Ecology* **14**, e2296 (2021).
67. Parazoo, N. C. et al. Detecting regional patterns of changing CO₂ flux in Alaska. *Proc. Natl Acad. Sci. USA* **113**, 7733–7738 (2016).
68. Silva, J. L. A., Souza, A. F., Caliman, A., Voigt, E. L. & Lichstein, J. E. Weak whole-plant trait coordination in a seasonally dry South American stressful environment. *Ecol. Evol.* **8**, 4–12 (2018).
69. Ward, C. P. & Cory, R. M. Chemical composition of dissolved organic matter draining permafrost soils. *Geochim. Cosmochim. Acta* **167**, 63–79 (2015).
70. Johnston, E. R. et al. Responses of tundra soil microbial communities to half a decade of experimental warming at two critical depths. *Proc. Natl Acad. Sci. USA* **116**, 15096–15105 (2019).
71. Stein, L. Y. The long-term relationship between microbial metabolism and greenhouse gases. *Trends Microbiol.* **28**, 500–511 (2020).
72. Feng, J. et al. Warming-induced permafrost thaw exacerbates tundra soil carbon decomposition mediated by microbial community. *Microbiome* **8**, 3 (2020).
73. Estop-Aragónes, C. et al. Assessing the potential for mobilization of old soil carbon after permafrost thaw: a synthesis of ¹⁴C measurements from the northern permafrost region. *Glob. Biogeochem. Cycles* **34**, e2020GB006672 (2020).
74. Wik, M., Varner, R. K., Anthony, K. W., MacIntyre, S. & Bastviken, D. Climate-sensitive northern lakes and ponds are critical components of methane release. *Nat. Geosci.* **9**, 99–105 (2016).
75. Schaefer, K., Lantuit, H., Romanovsky, V. E., Schuur, E. A. G. & Witt, R. The impact of the permafrost carbon feedback on global climate. *Environ. Res. Lett.* **9**, 085003 (2014).
76. Xue, K. et al. Tundra soil carbon is vulnerable to rapid microbial decomposition under climate warming. *Nat. Clim. Chang.* **6**, 595–600 (2016).
77. Bay, S. K. et al. Trace gas oxidizers are widespread and active members of soil microbial communities. *Nat. Microbiol.* **6**, 246–256 (2021).
78. Singleton, C. M. et al. Methanotrophy across a natural permafrost thaw environment. *ISME J.* **12**, 2544–2558 (2018).
79. Kwon, M. J. et al. Plants, microorganisms, and soil temperatures contribute to a decrease in methane fluxes on a drained Arctic floodplain. *Glob. Chang. Biol.* **23**, 2396–2412 (2017).
80. Jin, X.-Y. et al. Impacts of climate-induced permafrost degradation on vegetation: a review. *Adv. Clim. Chang. Res.* **12**, 29–47 (2020).
81. Song, X. et al. Soil moisture as a key factor in carbon release from thawing permafrost in a boreal forest. *Geoderma* **357**, 113975 (2020).
82. Zhu, Y. et al. Disproportionate increase in freshwater methane emissions induced by experimental warming. *Nat. Clim. Chang.* **10**, 685–690 (2020).
83. Watts, J. D., Kimball, J. S., Bartsch, A. & McDonald, K. C. Surface water inundation in the boreal-Arctic: potential impacts on regional methane emissions. *Environ. Res. Lett.* **9**, 075001 (2014).
84. Thompson, R. L. et al. Methane fluxes in the high northern latitudes for 2005–2013 estimated using a Bayesian atmospheric inversion. *Atmos. Chem. Phys.* **17**, 3553–3572 (2017).
85. Oh, Y. et al. Reduced net methane emissions due to microbial methane oxidation in a warmer Arctic. *Nat. Clim. Chang.* **10**, 317–321 (2020).
86. Street, L. E. et al. Plant carbon allocation drives turnover of old soil organic matter in permafrost tundra soils. *Glob. Chang. Biol.* **26**, 4559–4571 (2020).
87. Natali, S. M. et al. Large loss of CO₂ in winter observed across the northern permafrost region. *Nat. Clim. Chang.* **9**, 852–857 (2019).
88. Hu, Y., Fernandez-Anez, N., Smith, T. E. L. & Rein, G. Review of emissions from smouldering peat fires and their contribution to regional haze episodes. *Int. J. Wildland Fire* **27**, 293–312 (2018).
89. Abbott, B. W. et al. Biomass offsets little or none of permafrost carbon release from soils, streams, and wildfire: an expert assessment. *Environ. Res. Lett.* **11**, 034014 (2016).
90. Mack, M. C. et al. Carbon loss from boreal forest wildfires offset by increased dominance of deciduous trees. *Science* **372**, 280–283 (2021).
91. Holloway, J. E. et al. Impact of wildfire on permafrost landscapes: a review of recent advances and future prospects. *Permafrost Periglacial Process.* **31**, 371–382 (2020).
92. McCarty, J. L., Smith, T. E. L. & Turetsky, M. R. Arctic fires re-emerging. *Nat. Geosci.* **13**, 658–660 (2020).
93. Scholten, R. C., Jandt, R., Miller, E. A., Rogers, B. M. & Veraverbeke, S. Overwintering fires in boreal forests. *Nature* **593**, 399–404 (2021).
94. Koven, C. D. et al. A simplified, data-constrained approach to estimate the permafrost carbon-climate feedback. *Phil. Trans. R. Soc. A* **373**, 20140423 (2015).
95. MacDougall, A. H. & Knutti, R. Projecting the release of carbon from permafrost soils using a perturbed parameter ensemble modelling approach. *Biogeosciences* **13**, 2123–2136 (2016).
96. Cooper, M. D. A. et al. Limited contribution of permafrost carbon to methane release from thawing peatlands. *Nat. Clim. Chang.* **7**, 507–511 (2017).
97. Andresen, C. G. et al. Soil moisture and hydrology projections of the permafrost region—a model intercomparison. *Cryosphere* **14**, 445–459 (2020).
98. Bartsch, A., Pointner, G., Ingeman-Nielsen, T. & Lu, W. Towards circumpolar mapping of Arctic settlements and infrastructure based on Sentinel-1 and Sentinel-2. *Remote Sens.* **12**, 2368 (2020).
99. Swingedouw, D. et al. Early warning from space for a few key tipping points in physical, biological, and social-ecological systems. *Surv. Geophys.* **41**, 1237–1284 (2020).
100. Elder, C. D. et al. Airborne mapping reveals emergent power law of Arctic methane emissions. *Geophys. Res. Lett.* **47**, e2019GL085707 (2020).
101. Byrne, B. et al. Improved constraints on northern extratropical CO₂ fluxes obtained by combining surface-based and space-based atmospheric CO₂ measurements. *J. Geophys. Res. Atmos.* **125**, e2019JD032029 (2020).
102. Karlson, M. et al. Delineating northern peatlands using Sentinel-1 time series and terrain indices from local and regional digital elevation models. *Remote Sens. Environ.* **231**, 111252 (2019).

103. Cusworth, D. H. et al. Synthesis of methane observations across scales: strategies for deploying a multitiered observing network. *Geophys. Res. Lett.* **47**, e2020GL087869 (2020).
104. Bale, N. J. et al. Fatty acid and hopanoid adaption to cold in the methanotroph methylolulum psychrotolerans. *Front. Microbiol.* **10**, 589 (2019).
105. Mackelprang, R. et al. Microbial survival strategies in ancient permafrost: insights from metagenomics. *ISME J.* **11**, 2305–2318 (2017).
106. Siliakus, M. F., van der Oost, J. & Kengen, S. W. M. Adaptations of archaeal and bacterial membranes to variations in temperature, pH and pressure. *Extremophiles* **21**, 651–670 (2017).
107. Johnson, S. S. et al. Ancient bacteria show evidence of DNA repair. *Proc. Natl Acad. Sci. USA* **104**, 14401–14405 (2007).
108. Hueffer, K., Drown, D., Romanovsky, V. & Hennessy, T. Factors contributing to anthrax outbreaks in the circumpolar north. *Ecohealth* **17**, 174–180 (2020).
109. Miner, K. R. et al. Emergent biogeochemical risks from Arctic permafrost degradation. *Nat. Clim. Chang.* **11**, 809–819 (2021).
110. Perron, G. G. et al. Functional characterization of bacteria isolated from ancient Arctic soil exposes diverse resistance mechanisms to modern antibiotics. *PLoS ONE* **10**, e0069533 (2015).
111. Mackelprang, R. et al. Metagenomic analysis of a permafrost microbial community reveals a rapid response to thaw. *Nature* **480**, 368–371 (2011).
112. Burkert, A., Douglas, T. A., Waldrop, M. P. & Mackelprang, R. Changes in the active, dead, and dormant microbial community structure across a pleistocene permafrost chronosequence. *Appl. Environ. Microbiol.* **85**, e02646-18 (2019).
113. Jansson, J. K. & Hofmckel, K. S. Soil microbiomes and climate change. *Nat. Rev. Microbiol.* **18**, 35–46 (2020).
114. Hultman, J. et al. Multi-omics of permafrost, active layer and thermokarst bog soil microbiomes. *Nature* **521**, 208–212 (2015).
115. Schadel, C. et al. Potential carbon emissions dominated by carbon dioxide from thawed permafrost soils. *Nat. Clim. Chang.* **6**, 950–953 (2016).
116. Lee, H. et al. A spatially explicit analysis to extrapolate carbon fluxes in upland tundra where permafrost is thawing. *Glob. Chang. Biol.* **17**, 1379–1393 (2011).
117. Euskirchen, E. S., Edgar, C. W., Turetsky, M. R., Waldrop, M. P. & Harden, J. W. Differential response of carbon fluxes to climate in three peatland ecosystems that vary in the presence and stability of permafrost. *J. Geophys. Res. Biogeosci.* **119**, 1576–1595 (2014).
118. Euskirchen, E. S., Bret-Harte, M. S., Shaver, G. R., Edgar, C. W. & Romanovsky, V. E. Long-term release of carbon dioxide from arctic tundra ecosystems in Alaska. *Ecosystems* **20**, 960–974 (2017).
119. Karlsson, J. et al. Carbon emission from Western Siberian inland waters. *Nat. Commun.* **12**, 825 (2021).
120. Schuur, E. A. G. et al. Tundra underlain by thawing permafrost persistently emits carbon to the atmosphere over 15 years of measurements. *J. Geophys. Res. Biogeosci.* **126**, e2020JG006044 (2021).
121. Oechel, W. C. et al. Acclimation of ecosystem CO₂ exchange in the Alaskan Arctic in response to decadal climate warming. *Nature* **406**, 978–981 (2000).
122. Heijmans, M. M. P. D. et al. Tundra vegetation change and impacts on permafrost. *Nat. Rev. Earth Environ.* <https://doi.org/10.1038/s43017-021-00233-0> (2022).
123. Kanevskiy, M. et al. Patterns and rates of riverbank erosion involving ice-rich permafrost (yedoma) in northern Alaska. *Geomorphology* **253**, 370–384 (2016).
124. Pastorello, G. et al. The FLUXNET2015 dataset and the ONEFlux processing pipeline for eddy covariance data. *Sci. Data* **7**, 225 (2020).
125. Schimel, D. & Schneider, F. D. Flux towers in the sky: global ecology from space. *New Phytol.* **224**, 570–584 (2019).
126. Humphrey, V. et al. Soil moisture–atmosphere feedback dominates land carbon uptake variability. *Nature* **592**, 65–69 (2021).
127. Jammot, M. et al. Year-round CH₄ and CO₂ flux dynamics in two contrasting freshwater ecosystems of the subarctic. *Biogeosciences* **14**, 5189–5216 (2017).
128. Kohnert, K., Serafimovich, A., Metzger, S., Hartmann, J. & Sachs, T. Strong geologic methane emissions from discontinuous terrestrial permafrost in the Mackenzie Delta, Canada. *Sci. Rep.* **7**, 5828 (2017).
129. Sayres, D. S. et al. Arctic regional methane fluxes by ecotope as derived using eddy covariance from a low-flying aircraft. *Atmos. Chem. Phys.* **17**, 8619–8633 (2017).
130. Ueyama, M. et al. Upscaling terrestrial carbon dioxide fluxes in Alaska with satellite remote sensing and support vector regression. *J. Geophys. Res. Biogeosci.* **118**, 1266–1281 (2013).
131. Davidson, S. J. et al. Upscaling CH₄ fluxes using high-resolution imagery in Arctic tundra ecosystems. *Remote Sens.* **9**, 1227 (2017).
132. Peltola, O. et al. Monthly gridded data product of northern wetland methane emissions based on upscaling eddy covariance observations. *Earth Syst. Sci. Data* **11**, 1263–1289 (2019).
133. Chang, R. Y. W. et al. Methane emissions from Alaska in 2012 from CARVE airborne observations. *Proc. Natl Acad. Sci. USA* **111**, 16694–16699 (2014).
134. Saeki, T. et al. Carbon flux estimation for Siberia by inverse modeling constrained by aircraft and tower CO₂ measurements. *J. Geophys. Res. Atmos.* **118**, 1100–1122 (2013).
135. Kim, J. et al. Impact of Siberian observations on the optimization of surface CO₂ flux. *Atmos. Chem. Phys.* **17**, 2881–2899 (2017).
136. O’Shea, S. J. et al. Methane and carbon dioxide fluxes and their regional scalability for the European Arctic wetlands during the MAMM project in summer 2012. *Atmos. Chem. Phys.* **14**, 13159–13174 (2014).
137. Gottwald, M. & Bovensmann, H. *SCIAMACHY — Exploring the Changing Earth’s Atmosphere* (Springer, 2011).
138. Siewert, M. B. High-resolution digital mapping of soil organic carbon in permafrost terrain using machine learning: a case study in a sub-Arctic peatland environment. *Biogeosciences* **15**, 1663–1682 (2018).
139. Arndt, K. A. et al. Arctic greening associated with lengthening growing seasons in Northern Alaska. *Environ. Res. Lett.* **14**, 125018 (2019).
140. Widhalm, B., Bartsch, A. & Heim, B. A novel approach for the characterization of tundra wetland regions with C-band SAR satellite data. *Int. J. Remote Sens.* **36**, 5537–5556 (2015).
141. Varon, D. J. et al. High-frequency monitoring of anomalous methane point sources with multispectral Sentinel-2 satellite observations. *Atmos. Meas. Tech.* **14**, 2771–2785 (2021).
142. Bartsch, A., Hofer, A., Kroisleitner, C. & Trofaier, A. M. Land cover mapping in northern high latitude permafrost regions with satellite data: achievements and remaining challenges. *Remote Sens.* **8**, 979 (2016).
143. Flato, G. et al. in *Climate Change 2013: The Physical Science Basis. Contribution of Working Group I to the Fifth Assessment Report of the Intergovernmental Panel on Climate Change* Ch. 9 (eds Stocker, T. F. et al.) (Cambridge Univ. Press, 2013).
144. Kivimäki, E. et al. Evaluation and analysis of the seasonal cycle and variability of the trend from GOSAT methane retrievals. *Remote Sens.* **11**, 882 (2019).
145. Lindqvist, H. et al. Does GOSAT capture the true seasonal cycle of carbon dioxide? *Atmos. Chem. Phys.* **15**, 13023–13040 (2015).
146. Chadburn, S. et al. Carbon stocks and fluxes in the high latitudes: using site-level data to evaluate Earth system models. *Biogeosciences* **14**, 5143–5169 (2017).
147. Graven, H. D. et al. Enhanced seasonal exchange of CO₂ by northern ecosystems since 1960. *Science* **341**, 1085–1089 (2013).
148. Aas, K. S. et al. Thaw processes in ice-rich permafrost landscapes represented with laterally coupled tiles in a land surface model. *Cryosphere* **13**, 591–609 (2019).
149. Westermann, S. et al. Transient modeling of the ground thermal conditions using satellite data in the Lena River delta, Siberia. *Cryosphere* **11**, 1441–1463 (2017).
150. Houweling, S. et al. An intercomparison of inverse models for estimating sources and sinks of CO₂ using GOSAT measurements. *J. Geophys. Res.* **120**, 5253–5266 (2015).
151. Houweling, S. et al. Global inverse modeling of CH₄ sources and sinks: an overview of methods. *Atmos. Chem. Phys.* **17**, 235–256 (2017).
152. Tsuruta, A. et al. Global methane emission estimates for 2000–2012 from CarbonTracker Europe-CH₄ v1.0. *Geosci. Model Dev.* **10**, 1261–1289 (2017).
153. Virkkala, A. M., Abdi, A. M., Luoto, M. & Metcalfe, D. B. Identifying multidisciplinary research gaps across Arctic terrestrial gradients. *Environ. Res. Lett.* **14**, 124061 (2019).
154. Hakkarainen, J., Ialongo, I., Maksyutov, S. & Crisp, D. Analysis of four years of global XCO₂ anomalies as seen by Orbiting Carbon Observatory-2. *Remote Sens.* **11**, 850 (2019).
155. Fisher, J. B. et al. Missing pieces to modeling the Arctic-Boreal puzzle. *Environ. Res. Lett.* **13**, 020202 (2018).
156. McGuire, A. D. et al. An assessment of the carbon balance of Arctic tundra: comparisons among observations, process models, and atmospheric inversions. *Biogeosciences* **9**, 3185–3204 (2012).
157. Lenton, T. M. & Williams, H. T. P. On the origin of planetary-scale tipping points. *Trends Ecol. Evol.* **28**, 380–382 (2013).
158. Lenton, T. M. Arctic climate tipping points. *Ambio* **41**, 10–22 (2012).
159. Lenton, T. M. et al. Climate tipping points — too risky to bet against. *Nature* **575**, 592–595 (2019).
160. Fleisher, A. J., Long, D. A., Liu, Q., Gameson, L. & Hodges, J. T. Optical measurement of radiocarbon below unity fraction modern by linear absorption spectroscopy. *J. Phys. Chem. Lett.* **8**, 4550–4556 (2017).
161. Genoud, G. et al. Laser spectroscopy for monitoring of radiocarbon in atmospheric samples. *Anal. Chem.* **91**, 12315–12320 (2019).
162. Levin, I. et al. Observations and modelling of the global distribution and long-term trend of atmospheric ¹⁴CO₂. *Tellus B Chem. Phys. Meteorol.* **62**, 26–46 (2010).
163. Voigt, C. et al. Warming of subarctic tundra increases emissions of all three important greenhouse gases — carbon dioxide, methane, and nitrous oxide. *Glob. Chang. Biol.* **23**, 3121–3138 (2017).
164. Mu, C. C. et al. Permafrost collapse shifts alpine tundra to a carbon source but reduces N₂O and CH₄ release on the northern Qinghai-Tibetan Plateau. *Geophys. Res. Lett.* **44**, 8945–8952 (2017).
165. Krogh, S. A., Pomeroy, J. W. & Marsh, P. Diagnosis of the hydrology of a small Arctic basin at the tundra-taiga transition using a physically based hydrological model. *J. Hydrol.* **550**, 685–703 (2017).
166. Burke, E. J., Zhang, Y. & Krinner, G. Evaluating permafrost physics in the Coupled Model Intercomparison Project 6 (CMIP6) models and their sensitivity to climate change. *Cryosphere* **14**, 3155–3174 (2020).
167. Treat, C. C., Bloom, A. A. & Marushchak, M. E. Nongrowing season methane emissions — a significant component of annual emissions across northern ecosystems. *Glob. Chang. Biol.* **24**, 3331–3343 (2018).
168. Kelley, J. J., Weaver, D. F. & Smith, B. P. The variation of carbon dioxide under the snow in the Arctic. *Ecology* **49**, 358–361 (1968).
169. Du, J. et al. Assessing global surface water inundation dynamics using combined satellite information from SMAP, AMSR2 and Landsat. *Remote Sens. Environ.* **213**, 1–17 (2018).
170. Webb, E. E. et al. Increased wintertime CO₂ loss as a result of sustained tundra warming. *J. Geophys. Res. Biogeosci.* **121**, 249–265 (2016).
171. Grosse, G., Goetz, S., McGuire, A. D., Romanovsky, V. E. & Schuur, E. A. G. Changing permafrost in a warming world and feedbacks to the Earth system. *Environ. Res. Lett.* **11**, 040201 (2016).
172. Kleinen, T. & Brovkin, V. Pathway-dependent fate of permafrost region carbon. *Environ. Res. Lett.* **13**, 094001 (2018).
173. Anthony, K. M. W. et al. A shift of thermokarst lakes from carbon sources to sinks during the Holocene epoch. *Nature* **511**, 452–456 (2014).
174. Crichton, K. A., Bouttes, N., Roche, D. M., Chappellaz, J. & Krinner, G. Permafrost carbon as a missing link to explain CO₂ changes during the last deglaciation. *Nat. Geosci.* **9**, 683–686 (2016).
175. Tesi, T. et al. Massive remobilization of permafrost carbon during post-glacial warming. *Nat. Commun.* **7**, 13653 (2016).
176. McClain, M. E. et al. Biogeochemical hot spots and hot moments at the interface of terrestrial and aquatic ecosystems. *Ecosystems* **6**, 301–312 (2003).
177. Bernhardt, E. S. et al. Control points in ecosystems: moving beyond the hot spot hot moment concept. *Ecosystems* **20**, 665–682 (2016).
178. Kuze, A. et al. Update on GOSAT TANSO-FTS performance, operations, and data products after more than 6 years in space. *Atmos. Meas. Tech.* **9**, 2445–2461 (2016).
179. Eldering, A. et al. The Orbiting Carbon Observatory-2 early science investigations of regional carbon dioxide fluxes. *Science* **358**, eaam5745 (2017).

180. Yang, D. et al. First global carbon dioxide maps produced from TanSat measurements. *Adv. Atmos. Sci.* **35**, 621–623 (2018).
181. Glumb, R., Davis, G. & Lietzke, C. in *IEEE International Geoscience and Remote Sensing Symposium* 1238–1240 (IEEE, 2014).
182. Lorente, A. et al. Methane retrieved from TROPOMI: improvement of the data product and validation of the first 2 years of measurements. *Atmos. Meas. Tech.* **14**, 665–684 (2021).
183. Ehret, G. et al. MERLIN: a French–German space lidar mission dedicated to atmospheric methane. *Remote Sens.* **9**, 1052 (2017).
184. Bousquet, P. et al. Error budget of the Methane Remote Lidar mission and its impact on the uncertainties of the global methane budget. *J. Geophys. Res. Atmos.* **123**, 11,766–11,785 (2018).
185. Bezy, J.-L. et al. in *IEEE International Geoscience and Remote Sensing Symposium* 8400–8403 (IEEE, 2019).
186. Ingmann, P. et al. Requirements for the GMES atmosphere service and ESA's implementation concept: Sentinels-4/-5 and -5p. *Remote Sens. Environ.* **120**, 58–69 (2012).
187. Nassar, R. et al. The atmospheric imaging mission for northern regions: AIM-North. *Can. J. Remote Sens.* **45**, 423–442 (2019).
188. Polonsky, I. N., O'Brien, D. M., Kumer, J. B., O'Dell, C. W. & the geoCARB Team. Performance of a geostationary mission, geoCARB, to measure CO₂, CH₄ and CO column-averaged concentrations. *Atmos. Meas. Tech.* **7**, 959–981 (2014).
189. Chahine, M. T. et al. Improving weather forecasting and providing new data on greenhouse gases. *Bull. Am. Meteorol. Soc.* **87**, 911–926 (2006).
190. Clerbaux, C. et al. Monitoring of atmospheric composition using the thermal infrared IASI/MetOp sounder. *Atmos. Chem. Phys.* **9**, 6041–6054 (2009).
191. Han, Y. et al. Suomi NPP CrIS measurements, sensor data record algorithm, calibration and validation activities, and record data quality. *J. Geophys. Res. Atmos.* **118**, 734–12,748 (2013).
192. Zou, C. Z. et al. The reprocessed Suomi NPP satellite observations. *Remote Sens.* **12**, 2891 (2020).
193. Obu, J. et al. ESA Permafrost Climate Change Initiative (Permafrost_CCI): permafrost climate research data package v1 (CEDA, 2020).
194. Voigt, C. et al. Nitrous oxide emissions from permafrost-affected soils. *Nat. Rev. Earth Environ.* **1**, 420–434 (2020).
195. Arctic Climate Impact Assessment. *Impacts of a Warming Arctic: Arctic Climate Impact Assessment* (Cambridge Univ. Press, 2004).

Acknowledgements

A portion of this work was carried out at the Jet Propulsion Laboratory, California Institute of Technology, under a contract with the National Aeronautics and Space Administration (80NM0018D0004). This work is part of the NASA-ESA Arctic Methane and Permafrost Challenge (AMPAC). J.T. acknowledges funding from the Academy of Finland (projects 312125, 337552).

Author contributions

All authors contributed to the writing and revision of this paper.

Competing interests

The authors declare no competing interests.

Peer review information

Nature Reviews Earth & Environment thanks Maija Marushchak, Joshua Dean and the other, anonymous, reviewer(s) for their contribution to the peer review of this work.

Publisher's note

Springer Nature remains neutral with regard to jurisdictional claims in published maps and institutional affiliations.

© Springer Nature Limited 2022